ISSN 1024-8560, Atmospheric and Oceanic Optics, 2015, Vol. 28, No. 3, pp. 202–208. © Pleiades Publishing, Ltd., 2015.
Original Russian Text © V.V. Belov, M.V. Tarasenkov, V.N. Abramochkin, V.V. Ivanov, A.V. Fedosov, Yu.V. Gridnev, V.O. Troitskii, V.A. Dimaki, 2014, published in Optika Atmosfery i Okeana.

OPTICAL WAVES PROPAGATION

Atmospheric Bistatic Communication Channels with Scattering. Part 2. Field Experiments in 2013

V. V. Belov[a, b], M. V. Tarasenkov[a, b], V. N. Abramochkin[a], V. V. Ivanov[a], A. V. Fedosov[a], Yu. V. Gridnev[a], V. O. Troitskii[a], and V. A. Dimaki[a]

[a] *V.E. Zuev Institute of Atmospheric Optics, Siberian Branch, Russian Academy of Sciences, pl. Akademika Zueva 1, Tomsk, 634055 Russia*

[b] *Tomsk National State University, pr. Lenina 36, Tomsk, 634050 Russia*

e-mail: belov@iao.ru; tmv@iao.ru; ya.wna@yandex.ru; ilvlvltomsk@mail.ru; yuri@iao.ru; qel@asd.iao.ru

Received February 19, 2014

Abstract—Results of field experiments on the influence of atmospheric conditions and some instrumental characteristics on the quality of information transfer in a bistatic optoelectronic communication system (OECS) operating in the visible wavelengths range are considered. The length of the atmospheric channel reached 17 km. Radiation of a copper bromide vapor laser with a wavelength of 510.6 nm was used as a signal source. It is shown that bistatic or over-the-horizon OECSs can operate both under the conditions of a cloudy and cloud-free atmosphere. Average values and standard deviations of communication errors were estimated under different atmospheric-optical conditions when some characteristics of individual instrumentation units varied.

Keywords: bistatic optoelectronic communication systems, field experiments, optical and meteorological state of the atmosphere

DOI: 10.1134/S1024856015030069

INTRODUCTION

In work [1] we considered general questions of arrangement of bistatic (over-the-horizon) optoelectronic communication systems (OECSs), substantiated the choice of the Monte Carlo method for the theoretical study of the range of their applicability for different optical-geometrical schemes and conditions of their operation, described a laboratory implementation of the experimental setup and presented an example of its tests in 2012 under real atmospheric conditions. In the summer-fall period of 2013, a series of field experiments was undertaken to assess the possibility and quality of information reception via bistatic optical communication channels for different atmospheric conditions and for varying geometrical parameters of the receiver-transmitter OECS scheme.

In this paper, we describe the instrumentation and conditions of these experiments, as well as their results.

INSTRUMENTATION AND OPTICAL-GEOMETRICAL CONDITIONS OF EXPERIMENTS

A block-diagram of the laboratory prototype of bistatic OECS is shown in [1, Fig. 3]. We used a copper bromide vapor laser as a source of radiation [2]; it was constructed at the Institute of Atmospheric Optics, Siberian Branch, Russian Academy of Sciences, and has the following characteristics: the radiation wavelength $\lambda = 510.6$ nm, pulse repetition rate $f = 11$ kHz, pulse duration $\Delta t = 30$ ns, power $P = 4$–10 W, beam diameter at the entrance to the atmosphere $\varnothing = 15$ mm; and radiation divergence $\Delta\nu = 0.06$ mrad.

The field-of-view angle of receiving telescope was 2°; a FEU-84 photomultiplier tube (PMT) was used as a photodetector. The optical axis of the receiving telescope intersected the optical axis of laser beam, and its slope relative to horizontal plane was defined by the angle α (Fig. 1).

The transmitting OECS was located in the northern tower of building "A" of Institute of Atmospheric Optics, Siberian Branch, Russian Academy of Sciences, at height $h_0 = 13$ m above the Earth's surface, or 173 m above sea level, the direction of laser beam axis was defined by the elevation angle θ, which was varied from 5 to 15°, and by the azimuth angle φ, which could vary in horizontal plane within ± 10° of the direction to the receiving OECS located at the distance $Y_N = 8.73$ km from the transmitting OECS (along a straight line). The laser information beam successively passed over city, Tom River, and the suburban zone, sequentially including cropland, living settlement, and forest massifs. The mobile receiving optoelectronic system could be placed at any point, accessible for motor

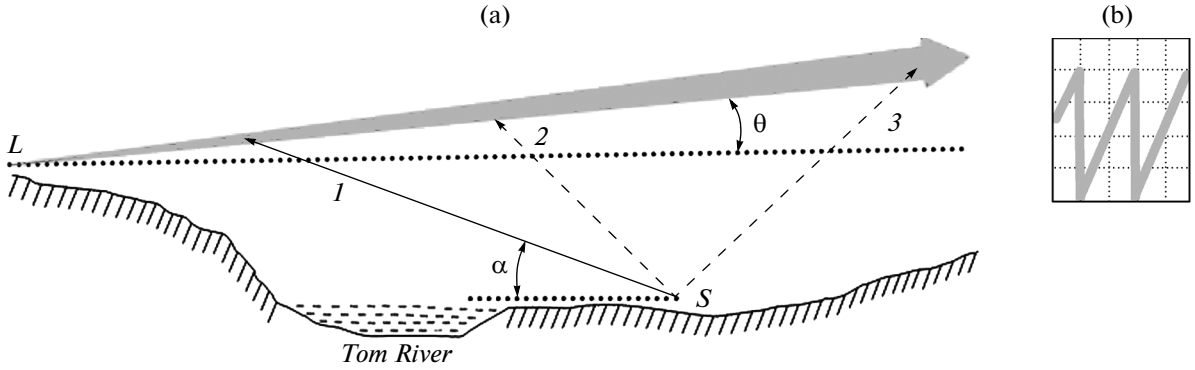

Fig. 1. (a) Geometry of experiments and (b) a fragment of test graphic signal.

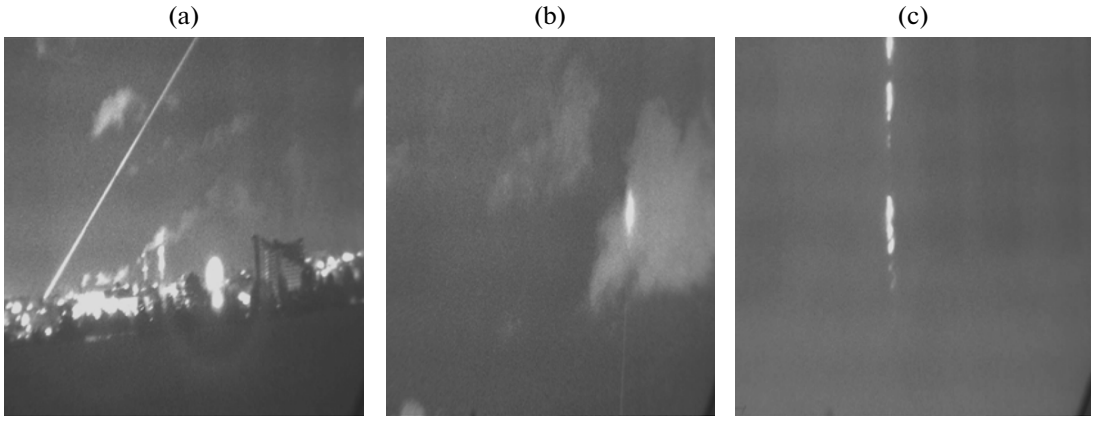

Fig. 2. Frames from video records of information-transmitting laser beam, (a) scattered over city; (b) scattered by a cloud system within the field-of-view of the receiver system; and (c) scattered by aerosol inhomogeneities within the field-of-view of the receiver system.

vehicles. The main experiments were performed for a fixed field location of the receiving system, indicated by symbol *S* in Fig. 1a (height above sea level was 80 m); also, the figure shows the general features of the profile of the Earth's surface below the laser beam, originating from point *L*. The length of the optical path was up to 11 km for position *2* (see Fig. 1), and up to 17 km for position *3*.

The experiments were performed in the period from August to October, 2013, at a dark time of the day under the conditions of cloudy (separate cloud systems, overcast clouds) and cloud-free atmosphere, and during rainfall. An image of the graphic test signal in the form of a periodic structure was used as information transferred via the atmospheric bistatic channel for a communication quality check (see Fig. 1b).

Each experiment was performed according to the following scheme. We fixed one of two orientations of the transmitting laser beam with angles $\theta \approx 5$ and 15° at $\varphi \approx 0°$. The receiver telescope was oriented in the directions *1* or *2* (see Fig. 1), corresponding to angles α from 15 to 85°. The telescope was oriented in the direction *3* (see Fig. 1) only when scattering at these points was recorded visually. Signal-transmitting radiation at $\varphi \approx \pm 10°$ was oriented selectively for communications checks. Depending on atmospheric conditions, each communication session for a fixed experiment geometry lasted from 7 to 30 min. It is noteworthy that information (graphic text), containing from 7000 to 40000 symbols, was transferred and saved in a computer. Sessions lasted from 30 min to 3 hr in each experiment.

As an example, Fig. 2 shows separate video images of the atmosphere-scattered laser radiation, recorded by the receiver system under different optical conditions in the atmosphere. In the case shown in Fig. 2a, the information was received by pointing the recording OECS at a specific region of the beam, and the atmospheric situation was cloud-free. Figure 2b shows the case with communication on the basis of the radiation scattered from cloud bottom boundary; and Fig. 2c shows situation with communication via scattering by

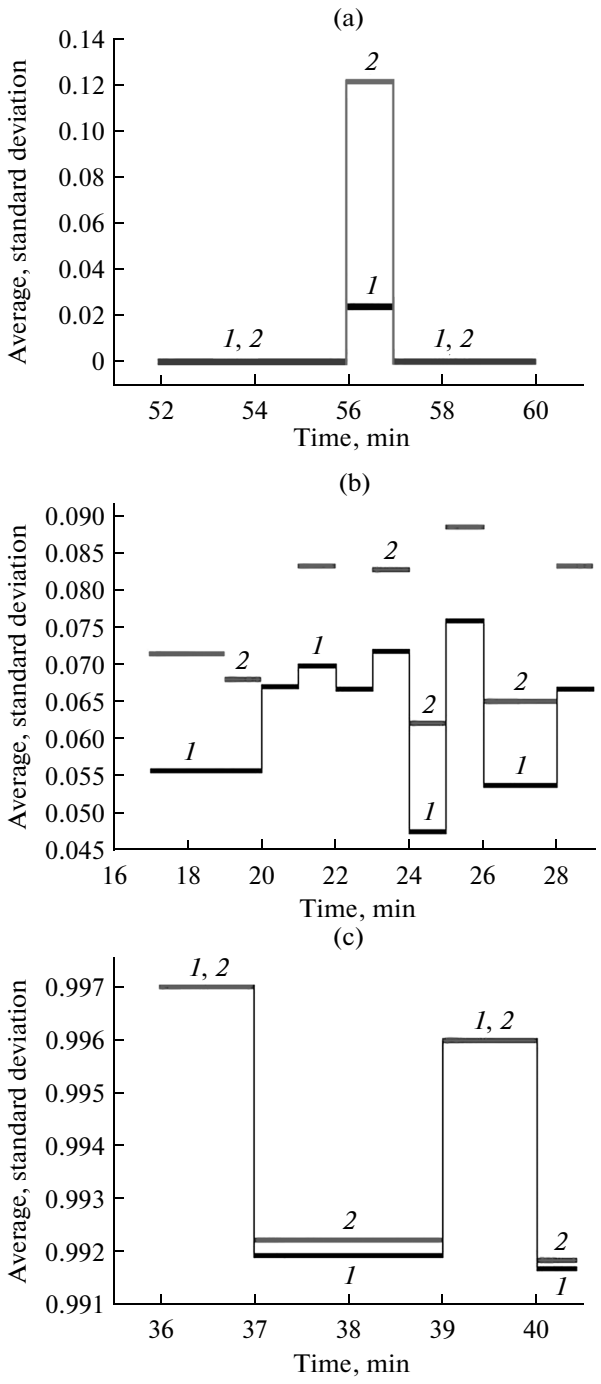

Fig. 3. Examples of communication quality characteristics: (a) communication session at 21:52–22:00 LT on September 11; (b) at 21:17–21:28 LT on September 25; (c) at 20:36–20:40 LT on September 29; average errors (*1*), and standard deviation (*2*).

aerosol inhomogeneities of cloud-free, but strongly turbid, atmosphere. Video was recorded with the help of the active-pulsed high-sensitivity ZOND+ OECS, which operated in passive mode. The ZOND+ system was created at the Institute of Atmospheric Optics, Siberian Branch, Russian Academy of Sciences and is a modification of the ZOND+ OECS [3].

The state of the atmospheric bistatic communication channel cannot be controlled under field conditions; therefore, the following parameters and means of their measurements were used to analyze the effect of optical and meteorological conditions on the quality of OECS operation. The meteorological visibility range S_M was measured every hour on the territory of the Basic Experimental Complex, Institute of Atmospheric Optics, Siberian Branch, Russian Academy of Sciences, located at a distance of 12 km from the point S (see Fig. 1). The range of S_M measurements was bounded above by $S_M = 30$ km. Pressure, humidity, and concentration of aerosol (with particle sizes larger than 0.3 μm) were measured at the TOR station [5], operating at the high-altitude station of the Institute of Atmospheric Optics, Siberian Branch, Russian Academy of Sciences, located 400 m away from the transmitter of the bistatic OECS. The aerosol extinction coefficient β^a_{ext} of the atmosphere at the wavelength $\lambda = 510.6$ nm was determined on a horizontal path, originating from the building where the transmitting OECS laser is placed; for this, the instrumentation and method described in [6–8] were used.

RESULTS OF EXPERIMENTS

The communication quality was estimated using the average value and standard deviation of the error over communication session, during which we recorded all geometrical parameters of the scheme of experiment (see Fig. 1). Let Z_i be the transmitted symbol, and z_i be the received symbol. We will assume that

$$x_i = \begin{cases} 0, \text{ if } Z_i = z_i \\ 1, \text{ if } Z_i \neq z_i \end{cases}. \quad (1)$$

Suppose that N symbols are transmitted during a communication session, so that

$$N = \sum_{j=1}^{m} n_j, \quad (2)$$

that is, the received series of symbols is divided into m packets, each consisting of n_j symbols. The average number of symbols, received erroneously, will be considered as a random quantity, i.e.,

$$y_j = \frac{1}{n_j} \sum_{i=1}^{n_j} x_i. \quad (3)$$

Then, the average symbol error rate during the channel transferring over a communication session is defined as

$$\bar{y} = \frac{1}{m} \sum_{j=1}^{m} y_j, \quad (4)$$

and the standard deviation is defined as

$$\bar{\sigma} = \sqrt{\frac{1}{m}\sum_{i=1}^{m} y_i^2 - \bar{y}^2}. \quad (5)$$

From statistical characteristics of information transfer quality, defined by formulas (1)–(5), it follows that error sources may be both atmospheric interference and changes in characteristics of receiver-transmitter optoelectronic modules (such as the power of laser radiation, PMT noises, etc.).

Analysis of average values of errors and their standard deviations showed that certain sessions had ideal communication quality, i.e., $\bar{y} = 0$ and $\bar{\sigma} = 0$ (such as on September 4) or near-ideal quality (such as on September 11); in other situations, the $\bar{y}$ values reached 0.8, and $\bar{\sigma}$ attained 0.9 (such as on September 29). Examples of these situations are shown in Fig. 3.

To clarify the reasons why the average errors $\bar{y}$ vary, we will turn to measurements of aerosol concentration, transmission coefficients, meteorological visibility range, temperature, humidity, and pressure in the near-ground atmospheric layer. The results of these measurements are shown in Fig. 4.

Since physical foundations for bistatic communication stem from the scattering effect, with contributions coming from both aerosol and molecular constituents of the atmosphere, it should be clarified first whether any one of the processes determines the communication quality or they are equally important in the series of experiments performed. For this, we will compare the molecular β_{sct}^{m} and aerosol β_{sct}^{a} scattering coefficients. The molecular scattering coefficients were calculated from formulas presented in [9] with the use of data on temperature and pressure, measured at the TOR station [5]. Considering that the aerosol extinction and scattering coefficients at a wavelength of 510.6 nm coincide with accuracy to within 90% (Table 1), Table 2 presents not β_{sct}^{a}, but rather the measured values of β_{ext}^{a}.

From Table 2 it follows that aerosol extinction (scattering) coefficients considerably (by almost an order of magnitude) exceed the molecular scattering coefficients, thus giving grounds to believe that it is just atmospheric aerosol constituents that determine the information transfer quality in bistatic OECSs on cloud-free paths, at least at a wavelength of 510.6 nm.

As was already indicated above, other error sources in information transfer via atmospheric communication channels may be changes in characteristics of individual instrumentation modules. With the chosen (time-pulse) method of information modulation, the information reception quality is influenced primarily by the power of laser radiation, which was varied in the range 4–10 W in the experiment; moreover, measurements were performed episodically. The less the power P, the worse the communication quality, i.e., the greater error rate $\bar{y}$ can be expected. As an example, this is confirmed by comparison of $\bar{y}$ values, obtained for the experiments performed on September 16, when $P = 6$ W, with those for September 25, when $P = 2$ W. In these experiments, $\bar{y} = 0.01$ and 0.572, respectively, air temperature was + 14.7°C on September 25 and – 4.3°C on September 16, the meteorological visibility range was $S_M > 30$ km on September 25 and 7 km on September 16, the measurement-derived aerosol extinction coefficient was $\beta_{ext}^{a} = 0.102$ km^{-1} at 21:00 LT on September 16 and $\beta_{ext}^{a} = 0.260$ km^{-1} on September 25.

Table 1. Aerosol scattering and extinction coefficients for different meteorological visibility ranges

S_M, km	β_{sct}^{a}, km^{-1}	β_{ext}^{a}, km^{-1}
1	4.1058	4.3317
2	2.0474	2.1603
5	0.81258	0.85747
10	0.39992	0.42206
15	0.26041	0.27485
25	0.14884	0.15712
50	0.06824	0.072029
99	0.02834	0.029914

Table 2. Aerosol extinction measurements inferred from measurements (superscript a) and molecular scattering coefficients (superscript m), calculated according to formulas in [10] versus day of year

Day of year	β_{ext}^{a}, km^{-1}	β_{sct}^{m}, km^{-1}
213	0.430	0.014857
214	0.224	0.015022
247	0.193	0.014923
248	0.083	0.01541
253	0.123	0.015305
254	0.084	0.015401
255	0.186	0.015836
259	0.102	0.015948
260	0.058	0.016009
262	0.103	0.015946
263	0.108	0.01605
265	0.105	0.016032
268	0.260	0.015224
272	0.106	0.016095
273	0.063	0.01591
275	0.163	0.015799

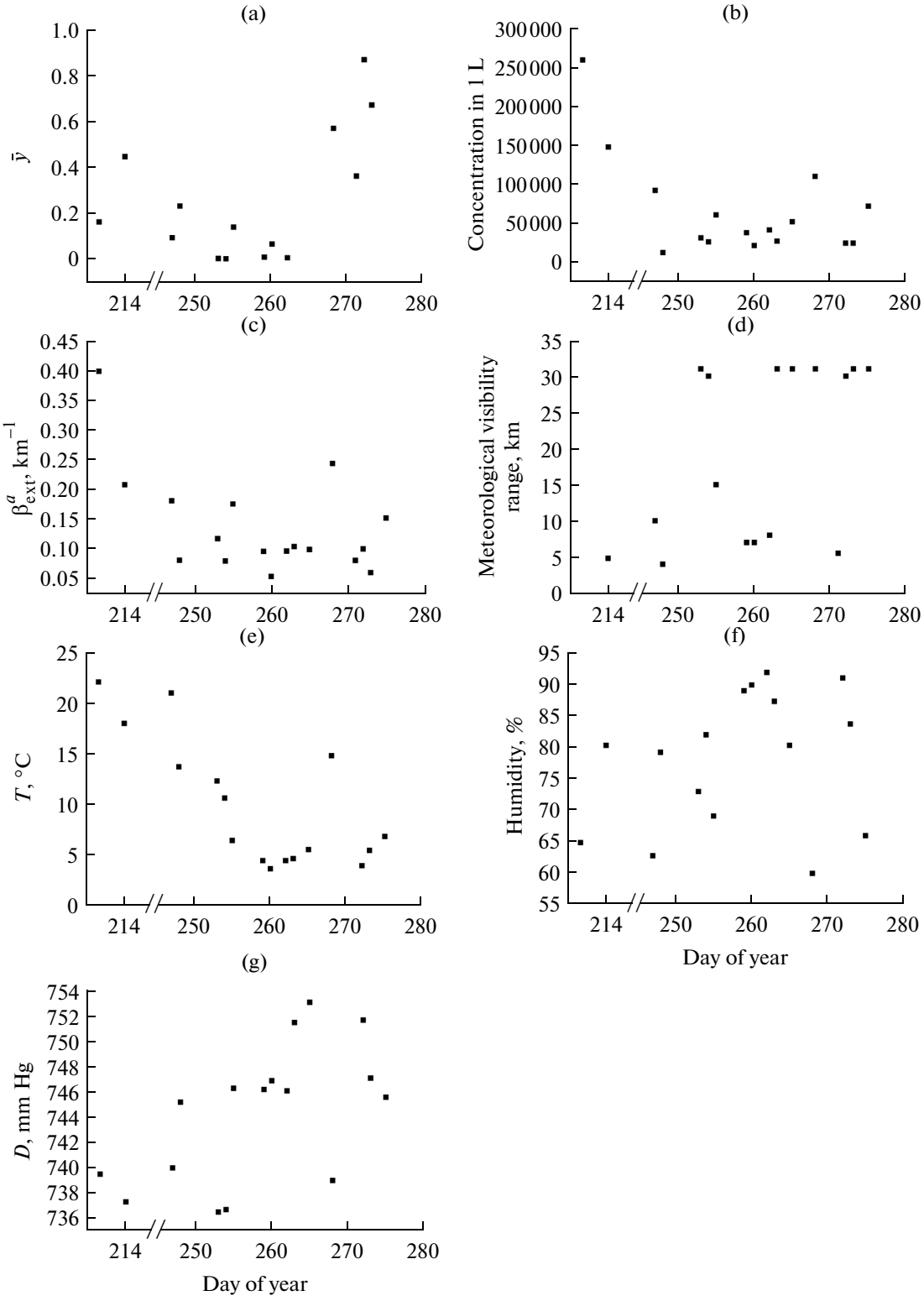

Fig. 4. (a) Average values $\bar{y}$, (b) aerosol concentration, (c) extinction coefficient, (d) meteorological visibility range, (e) temperature, (f) humidity, and (g) pressure for each day of experiments performed according to the scheme in Fig. 1.

Table 3. Sampling averages and standard deviations of communication errors in experiments on October 1, 2013

Time	$\bar{y}$	$\bar{\sigma}$	Time	$\bar{y}$	$\bar{\sigma}$	Time	$\bar{y}$	$\bar{\sigma}$
20:35	0.538	0.565	20:55	0.053	0.065	21:08	0.043	0.060
20:36	0.277	0.308	20:56	0.046	0.059	21:09	0.035	0.069
20:37	0.221	0.252	20:57	0.054	0.065	21:11	0.030	0.041
20:38	0.143	0.163	20:58	0.089	0.103	21:12	0.041	0.054
20:39	0.114	0.135	20:59	0.103	0.120	21:13	0.033	0.051
20:48	0.043	0.061	21:02	0.064	0.082	21:14	0.026	0.035
20:49	0.060	0.079	21:03	0.055	0.063	21:15	0.026	0.039
20:50	0.068	0.086	21:04	0.041	0.054	21:16	0.029	0.043
20:51	0.083	0.106	21:05	0.039	0.060	21:17	0.031	0.049
20:53	0.069	0.081	21:06	0.040	0.054	21:18	0.030	0.047
20:54	0.039	0.054	21:07	0.035	0.046	21:20	0.024	0.040

In this regard, before indicating the main reason for the rapid change in errors $\bar{y}$ (temperature, power of laser radiation, or aerosol extinction), we will consider the effect of PMT temperature on communication quality in the field experiments performed in 2013. This question can be answered by reference to Table 3, which presents the $\bar{y}$ and $\bar{\sigma}$ values for different periods of communication sessions.

The first session was performed without forced cooling of PMT; therefore, PMT temperature corresponded to the ambient temperature, i.e., $T = +6.7$°C (on October 2, 2014). The second and subsequent sessions were performed with the turned-on cooling installation which cooled the PMT down to temperature of −17°C for 30 min. As can be seen, the PMT temperature influences substantially the communication quality; and, as PMT temperature varies from +6.7°C to −17°C, the communication errors decrease by almost an order of magnitude. This result is not quite straightforward to interpret; although the relationship between temperature and characteristics (and, in particular, signal-to-noise ratio) has been long known [11].

CONCLUSIONS

Field experiments, performed during 2013 at the Institute of Atmospheric Optics, Siberian Branch, Russian Academy of Sciences, with the purpose of assessing the feasibility and quality of information transfer via bistatic OECSs, make it possible to draw the following general and specific conclusions.

1. High-quality bistatic optoelectronic communication in the visible wavelength range can be performed under the conditions of both a cloudy (see Fig. 3b) and clear-sky atmosphere (see Fig. 2a–c).

2. In the presence of clouds, communication can be performed through the regions of entrance and scattering of laser radiation at the overcast cloud bottom boundary or at the bottom or lateral boundaries of single clouds, or in the region of exit of radiation from the cloud (semitransparent clouds, see Fig. 2b).

3. The statistical characteristics of the quality of information transfer via bistatic atmospheric channels (average errors and their standard deviation) depend on the power of laser radiation (decreasing proportionally to the power growth) and on the PMT sensitivity. Cooling of the used FEU-84 in one of the experiments from +6.7 to −17°C had the result that the error rate decreased by almost an order of magnitude.

4. Analysis of how optical and meteorological states of the atmosphere influence the statistical characteristics of communication quality at a wavelength of 510.6 nm showed that, in bistatic communication schemes, when the laser beam is intercepted by the receiver system in the near-ground atmospheric layer, the communication quality is determined by scattering of radiation, which mainly depends on aerosol content in the atmosphere (see Fig. 4).

5. To eliminate or mitigate the effect of instrumentally caused failures of over-the-horizon OECSs, the method of field experiments should provide for a guaranteed stability of power of radiation transmitter and constant PMT temperature.

Our results will await further clarification in subsequent experimental and theoretical studies with the purpose of determining the key factors influencing the communication quality and range of bistatic OECSs with respect to optical-geometrical characteristics and parameters of its implementation schemes.

ACKNOWLEDGMENTS

The authors would like to thank B. D. Belan, M. V. Panchenko, V. N. Uzhegov, and T. K. Sklyadneva for providing data on the optical and meteorological state of the atmosphere, D. V. Belov for participation in experiments and for solving the problem of PMT cooling, A. N. Kudryavtsev for video record-

ing the variants of schemes for registering the information flows (see Fig. 2), and V. P. Protasova for technical processing of the work. This work was supported by State Contract no. 14.515.11.0030, Russian Foundation for Basic Research (grant no. 14-01-00211_A), Siberian Branch of the Russian Academy of Sciences (integration project no. 131a), and President of the Russian Federation (grant no. NSh-4714.2014.5 for support of leading scientific schools).

REFERENCES

1. V. V. Belov, M. V. Tarasenkov, V. N. Abramochkin, V. V. Ivanov, A. V. Fedosov, V. O. Troitskii, and D. V. Shiyanov, "Atmospheric bistatic communication channels with scattering. Part 1. Methods of study," Atmos. Ocean. Opt. **26** (5), 364–370 (2013).
2. V. A. Dimaki, V. B. Sukhanov, V. O. Troitskii, A. G. Filonov, and D. Yu. Shestakov, "A copper bromide vapor laser with computer control of the repetitive-pulse, train, and waiting operating modes," Instrum. Exp. Tech. **51** (6), 890–893 (2008).
3. V. V. Belov, G. G. Matvienko, R. Yu. Pak, D. V. Shiyanov, R. Yu. Kirpichenko, M. I. Kuryachii, I. N. Pustynskii, and Yu. A. Shurygin, "Active TV systems of vision with selection of scattering background," Datchiki Sist., No. 3, 25–30 (2012).
4. V. E. Zuev, B. D. Belan, and G. O. Zadde, *Optical Weather* (Nauka, Novosibirsk, 1990) [in Russian].
5. M. Yu. Arshinov, B. D. Belan, D. K. Davydov, G. A. Ivlev, A. V. Kozlov, D. A. Pestunov, E. V. Pokrovskii, G. N. Tolmachev, and A. V. Fofonov, "Sites for monitoring of greenhouse gases and gases oxidizing the atmosphere," Atmos. Ocean. Opt. **20** (1), 45–53 (2007).
6. Yu. A. Pkhalagov and V. N. Uzhegov, "Statistical method for decomposing total IR radiation attenuation coefficients," Opt. Atmos. **1** (10), 3–11 (1988).
7. Yu. A. Pkhalagov, V. N. Uzhegov, and N. N. Shchelkanov, "On aerosol–gas relationships in the ground layer of the atmosphere," Atmos. Ocean. Opt. **5** (6), 404–408 (1992).
8. V. N. Uzhegov, A. P. Rostov, and Yu. A. Pkhalagov, "Automated path photometer," Opt. Atmos. Okeana **26** (7), 590–594 (2013).
9. F. X. Kneizys, E. P. Shettle, G. P. Anderson, L. W. Abreu, J. H. Chetwynd, J. E. A. Selby, S. A. Clough, and W. O. Gallery, *User Guide to LOWTRAN-7. ARGL-TR-86-0177. ERP 1010* (Hansom AFB, Bedford, MA).
10. A. Bucholtz, "Rayleigh-scattering calculations for the terrestrial atmosphere," Appl. Opt. **34** (15), 2765–2773 (1995).
11. N. A. Soboleva and A. E. Melamid, *Photoelectronic Devices* (Vysshaya Shkola, Moscow, 1974) [in Russian].

Translated by O. Bazhenov